Tropical Easterly Waves in the Atlantic and East Pacific and their connections to the West African and Central American Monsoons

Connor M. DeLaune[1,2] (cmd23b@fsu.edu), V. Misra[1, 2], & C. B. Jayasankar[1]

[1]Center for Ocean-Atmospheric Prediction Studies, Florida State University, Tallahassee, Florida, USA

[2]Department of Earth, Ocean and Atmospheric Science, Florida State University, Tallahassee, Florida, USA

Introduction

- Tropical easterly waves (TEWs) are synoptic-scale inverted, Rossby Wave-like disturbances that propagate westward across the tropics.
- Globally, there are two maxima in TEW activity: West Africa and the Main Development Region (MDR) over the Atlantic and the northern East Pacific (Belanger et al. 2017).
- TEWs also propagates through two distinct monsoonal regions: West Africa and Central America.
- The onset dates of the West African (WAM) and Central American Monsoon (CAM) has significant influence over the location of the Intertropical Convergence Zone (ITCZ) along with the strength and location of the African Easterly Jet in the case of the WAM (Alfaro 2002; Sultan and Janicot 2003; Jayasankar and Misra 2025).
- This study aims to analyze how monsoon variations can influence the track density and structure of these TEWs across West Africa, the Atlantic, Central America, and the East Pacific.

Data and Methodology

- TEWs were identified using an objective tracking algorithm from Belanger et al. (2017) which used 5 criteria: (1) zonal winds are less than 2.5 m/s, (2) the curvature vorticity anomaly exceeded the 70th percentile of the climatology, (3) the advection of curvature vorticity is equal to 0 s-2, (4) the TEW lasted for at least 2 days, and (5) the median speed of the TEW is -25 m/s to -2 m/s to ensure westward propagation.



***Figure 1**: 850 mb curvature vorticity anomalies (contoured) and wind vectors on 3 July 2018 12z*

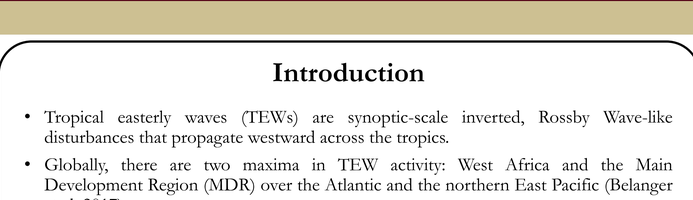


***Figure 2**: Masked 850 mb curvature vorticity anomalies using the 70th percentile of the ERA5 1986-2022 climatology on 3 July 2018 12z. The wind vectors are not masked, and the red lines represents TEWs that were identified after processing.*

- Five different reanalysis datasets were analyzed at 850 mb, 700 mb, and 600 mb across a domain extending from 100°W to 30°E and 0° to 25°N:
  - European Centre for Medium-Range Weather Forecasting (ECMWF) Reanalysis v5 (ERA5) from 1986-2022
  - Climate Forecasting System Reanalysis (CFS-R) from 1979-2010
  - ECMWF Reanalysis – Interim (ERA-Interim) from 1979-2010
  - ECMWF Reanalysis – 40 years (ERA-40) from 1965-2001
  - National Centers for Environmental Prediction-National Center for Atmospheric Research Reanalysis I (NCEP-NCAR) from 1974-2010
- The latter 4 datasets were extracted from the National Center for Environmental Information Tropical Easterly Wave Climatology Version 1.
- A filtering process was applied to the TEW datasets to remove waves with average trough-axis vorticity less than 1e-5 s^{-1}.
- For the monsoon variations, the Climate Hazards Group InfraRed Precipitation with Station data (CHIRPS) rainfall data from 1981-2022 was utilized to identify the onset of the WAM and CAM using the cumulative anomaly method from Misra and DiNapoli (2014).
- For the AEJ analysis, ERA5 was used to identify the average latitude of maximum wind speed at 600 mb from May-November for 1981-2022.

Results

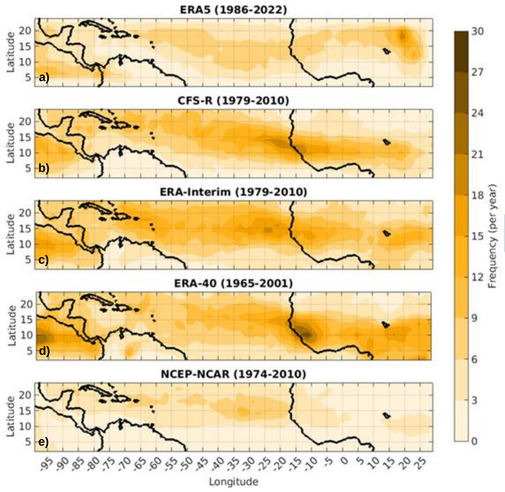


***Figure 3**: Average May-November TEW track densities at 700 mb for (a) ERA5 from 1986-2022, (b) CFS-R from 1979-2010, (c) ERA-Interim from 1979-2010, (d) ERA-40 from 1965-2001, and (e) NCEP-NCAR from 1974-2010.*

Filtering

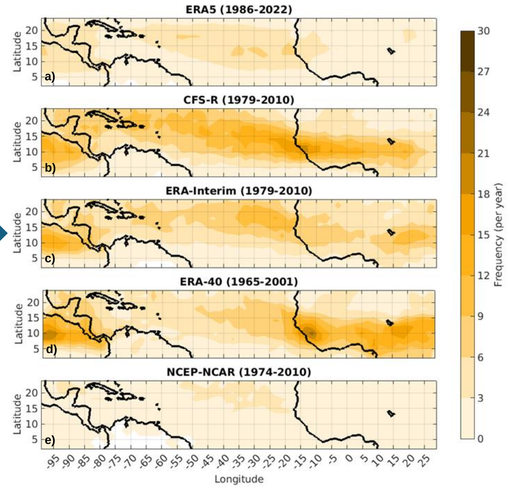


***Figure 4**: Average May-November TEW filtered track densities at 700 mb for (a) ERA5 from 1986-2022, (b) CFS-R from 1979-2010, (c) ERA-Interim from 1979-2010, (d) ERA-40 from 1965-2001, and (e) NCEP-NCAR from 1974-2010. TEWs are filtered by including only waves that exceed 1e-5 s^{-1}.*

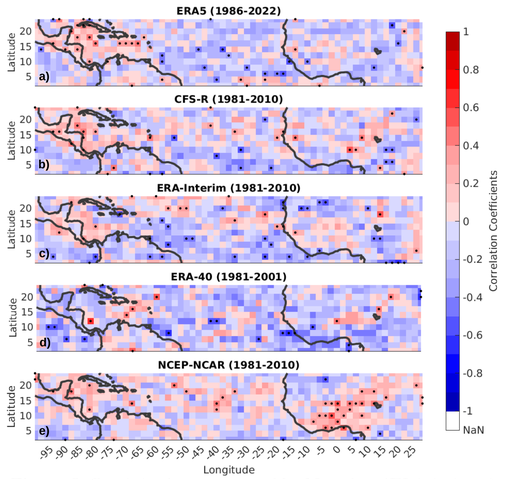


***Figure 5**: Correlation between average May-November AEJ latitude and the unfiltered May-November TEW track densities at 700 mb for (a) ERA5 from 1986-2022, (b) CFS-R from 1981-2010, (c) ERA-Interim from 1981-2010, (d) ERA-40 from 1981-2001, and (e) NCEP-NCAR from 1981-2010. The black dots represent regions with p-values less than 0.05.*

- Besides ERA-40, all the reanalysis datasets show that a northward displacement of the seasonal AEJ leads to more 700 mb TEWs in the western Caribbean.
- On average, the AEJ is zonally shorter when displaced to the north, limiting interaction times with TEWs. This can lead to weaker TEWs that do not recurve (Bercos-Hickey et al. 2020).
- The onset of the WAM influences the position of the AEJ at 600 mb as seen in Jayasankar and Misra (2025).
  - Early onset → Southward shift of AEJ
  - Late onset → Northward shift of AEJ
- However, correlations with the WAM onsets did not yield significant results.

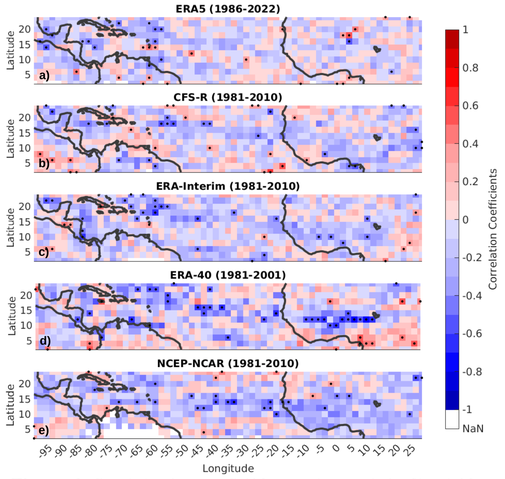


***Figure 6**: Correlation between CAM onset dates and the filtered May-November TEW track densities at 700 mb for (a) ERA5 from 1986-2022, (b) CFS-R from 1981-2010, (c) ERA-Interim from 1981-2010, (d) ERA-40 from 1981-2001, and (e) NCEP-NCAR from 1981-2010. The black dots represent regions with p-values less than 0.05.*

- All datasets have a significant negative correlation between the CAM onset and strong TEWs to the north and east of Puerto Rico and the Leeward Islands.
- These negative correlations also extend back towards the west coast of Africa but are not significant across the datasets.
- This indicates that an earlier onset of the CAM is associated with a greater number of strong TEWs that end up recurving over the Atlantic.
- There is also significant negative correlations to north and east of Central America except in NCEP-NCAR.
- This could be linked to the CAM influencing the Central American Gyre and local TEW generation.

Results (cont.)

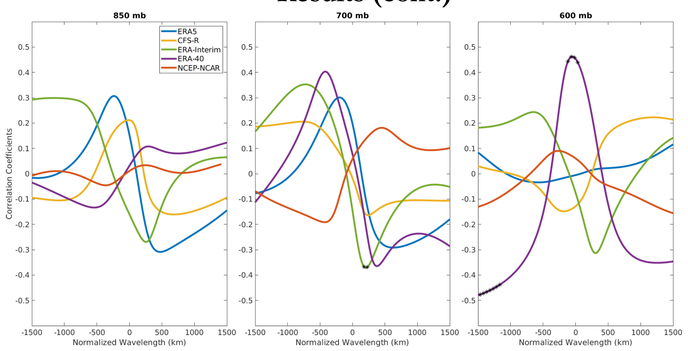


***Figure 7**: Correlation between WAM onset dates and the probability density functions of unfiltered TEW average wavelengths over the Atlantic and West Africa for each May-November season, normalized using the wavelength at the maximum average probability for each dataset. The black asterisks represent wavelengths with p-values less than 0.05.*

- Even though a small portion of the 700 mb correlations were significant, a pattern emerged from 4 of the 5 datasets with later onsets of the WAM (i.e., the positive correlations) being associated with shorter wavelengths while early onsets produced longer wavelengths.
- These findings can be tied back to the AEJ position and its influence on TEW intensity and structure.

Conclusions

- As shown in Belanger et al. (2017), TEW track densities are highly variable between reanalysis datasets, including ERA5.
- Filtering TEWs by a single vorticity threshold across datasets produced mixed effects on track densities.
- A northward displacement of the seasonal AEJ leads to more TEWs in the western Caribbean as seen 4 of the 5 datasets.
- Earlier CAM onset dates increases the possibility of strong TEWs recurving over the Atlantic.
  - The strength of the NASH needs to be analyzed as well.
- The CAM's influence on Central American Gyres need to be studied as earlier onsets are correlated with more, strong TEWs in the western Caribbean.
- Correlations between the onset of the WAM and TEW average wavelengths over Africa and the Atlantic did not yield significant results.
  - 700 mb TEWs had the most consistent results with 4 of the 5 datasets showing that early onsets of WAM led to shorter wavelengths while later onsets produced longer wavelengths.
- Correlations of TEW amplitude, vorticity, and precipitation with the WAM and CAM onsets will be examined in the future.

References

Alfaro, E. J., 2002: Some characteristics of the annual precipitation cycle in Central America and their relationship with its surrounding tropical oceans. *Top. Meteorol. Oceanogr.*, **9**, 88103.

Belanger, J. I., M. T. Jelinek, and J. A. Curry, 2017: A climatology of easterly waves in the tropical Western Hemisphere. *Geosci. Data J.*, **3**, 40–49.

Bercos-Hickey, E., T. R. Nathan, and S. Chen, 2020: On the Relationship between the African Easterly Jet, Saharan Mineral Dust Aerosols, and West African Precipitation. *J. Climate*, **33**, 3533–3546.

Jayasankar, C. B. and V. Misra, 2025: Seasonal outlook on the West African Rainy Season: Monitoring Onset Date Variations using GPM IMERG Satellite-based Precipitation. J. Hydromet. In review.

Misra, V., and S. DiNapoli, 2014: The variability of the Southeast Asian summer monsoon. *Int. J. Climatol.*, **34**(3), 893-901.

Sultan, B., and S. Janicot, 2003: The West African Monsoon Dynamics. Part II: The "Preonset" and "Onset" of the Summer Monsoon. *J. Climate*, **16**, 3407–3427.

Acknowledgement: The authors gratefully acknowledge the support given by NASA Grant 80NSSC22K0595.